Gas Permeation in Miscible Homopolymer–Copolymer Blends. I. Poly(methyl Methacrylate) and Styrene / Acrylonitrile Copolymers

J. S. CHIOU and D. R. PAUL, *Department of Chemical Engineering and Center for Polymer Research, University of Texas at Austin, Austin, Texas 78712*

Synopsis

Gas transport properties in homogeneous blends of PMMA with each of two SAN random copolymers, containing 13.5 and 28% by weight of acrylonitrile respectively, have been measured at 35°C for He, H_2, O_2, N_2, Ar, CH_4, and CO_2. For all cases, the permeability and diffusion coefficients are higher than that expected from the semilogarithmic additivity rule. On the other hand, the solubility coefficients and the ideal gas separation factors follow this rule well. These results for PMMA/SAN blends differ from those observed recently for other miscible blend systems; however, they agree well with recent theories proposed to describe gas sorption and permeation behavior in polymer mixtures. The composition dependence of gas transport properties observed in PMMA/SAN blends is attributed to the very weak net interactions between PMMA and SAN produced by repulsions between styrene and acrylonitrile units in the SAN random copolymers. Gas transport properties in phase-separated PMMA/SAN blends have also been studied. The phase-separated blends show sorption and permeation properties very similar to the corresponding homogeneous blends which can be explained by an isotropic, interconnected, two-phase model proposed by Kraus and Rollmann. Gas permeabilities for the solution cast PMMA films used here are compared with melt-extruded specimens used previously, and the differences are attributed to molecular orientation.

INTRODUCTION

Recent studies in our laboratory have shown that gas transport properties of miscible blends are affected by the extent of interaction between the component polymers.[1–10] For miscible blends with moderate interactions, gas permeability coefficients P are often lower than that calculated from the semilogarithmic additivity rule,[8,9] i.e.,

$$\ln P = \phi_1 \ln P_1 + \phi_2 \ln P_2 \tag{1}$$

where ϕ's are volume fractions and subscripts 1 and 2 refer to the two-component polymers. In one case reported where the interactions are quite weak,[4] permeabilities of the blends exactly follow eq. (1). When the interactions are stronger, permeabilities of the blends are significantly lower than that calculated by eq. (1) and in some cases are even lower than that of the two

Journal of Applied Polymer Science, Vol. 34, 1037–1056 (1987)
 CCC 0021-8995/87/031037-20$04.00

component polymers.[7,11] On the other hand, no cases have been reported to date where permeabilities are higher than that calculated by eq. (1), although this is the prediction of the following equation[9] derived from free volume theory[9,12] as the rule of mixtures for gas permeability in miscible blends or random copolymers:

$$\ln(P/A) = [\phi_1/\ln(P_1/A) + \phi_2/\ln(P_2/A)]^{-1} \quad (2)$$

for the case where there is no volume change on mixing, i.e., weak interaction. The term A is a characteristic constant for a specific gas. Contrary to the results observed to date for other miscible blends, gas permeabilities in a random copolymer of methacrylonitrile and styrene are well described by eq. 2.[13] These observations suggest that gas transport can be a useful probe to examine the interactions in multicomponent polymer systems.

Blends of poly(methyl methacrylate) (PMMA) with styrene/arylonitrile copolymers (SANs) are miscible over a limited range of SAN comonomer compositions (PMMA is not miscible with either homopolymer of styrene or acrylonitrile) and have been extensively studied.[14-21] The basis for miscibility in this blend system is the intramolecular repulsion between styrene and acrylonitrile units rather than any favorable interaction between PMMA and homopolymers of styrene or acylonitrile.[19] Since the net interaction of PMMA with SAN varies with comonomer composition, it is of interest to compare gas transport behavior of blends of PMMA with SANs of different acrylonitrile contents. However, all evidence to date including experimental measurement of densities, heat capacities, infrared spectra, dielectric relaxation, and calorimetry suggest that the absolute net interaction between PMMA and SAN is weak[17-19] even as the AN content is varied from the edge of the miscibility window to the optimum value.[21]

EXPERIMENTAL

Two styrene/acrylonitrile copolymers containing 13.5 and 28% by weight of acrylonitrile (AN) were separately mixed with poly(methyl methacrylate) to prepare blends. All three of these polymers are totally amorphous. Table I lists the abbreviations used, their densities, glass transition temperatures, molecular weights, and sources. The PMMA and SAN pellets in the desired ratio were dissolved in tetrahydrofuran (THF) to form solutions containing about 5% by weight of total polymer. The solutions were poured onto glass plates to cast films by allowing the solvent to evaporate slowly. The films were dried in an air circulating oven at 75°C for 1 week and then at 130°C for another week. After drying, the films were quenched to ambient temperature.

The gas permeation measurements were made using a high pressure permeation cell whose design and operation have been reported before.[22,23] Permeability coefficients for seven gases, He, H_2, O_2, N_2, Ar, CH_4, and CO_2, were measured at 35°C. The upstream side pressure was generally at 1–2 atm while the downstream side pressure was effectively zero. For N_2 and CH_4 with PMMA, the permeabilities were so low that higher driving pressures up to 3–5 atm were used to enhance the accuracy of measurement.

TABLE I
Polymers Used in This Study

Abbreviation	PMMA	SAN 28	SAN 13.5
Polymer	Poly(methyl methacrylate)	Styrene/acrylonitrile copolymer with 28% by weight of AN	Styrene/acrylonitrile copolymer with 13.5% by weight of AN
T_g (°C)	106	104	104
Density (g/cm^3)	1.188	1.080[a]	1.063[a]
Molecular weight (g/mol)	M_n = 52,900[b] M_w = 105,400	M_n = 88,600[c] M_w = 223,000 M_z = 679,600	Not available
Source	Rohm and Haas Plexiglas V(811)	Union Carbide RMD-4511	Asahi Chemical Industry Co., Ltd.

[a] Data from ref. 21.
[b] Provided by supplier.
[c] Data from ref. 14.

RESULTS AND DISCUSSION

Gas Permeation

As mentioned before, one objective of this study is to compare the composition dependence of gas transport properties of blends of PMMA with SAN copolymers having various AN contents. The criterion for the choice of SANs was based on the magnitude of their blend cloud points on heating. Phase separation on heating, i.e., lower critical solution temperature behavior, has been observed for miscible PMMA/SAN blends and their cloud points vary significantly with comonomer composition.[21] At a fixed ratio of PMMA to SAN, for example, 50/50, a maximum in the cloud point occurs beyond 400°C for SANs with 13–16% AN by weight in contrast to a value of approximately 200°C for SAN with about 30% AN. Since the magnitude of the cloud point may be taken as an indication of the extent of net interaction in the blend, the blends formed from the SAN of 13.5% AN content were chosen to represent PMMA/SAN blends having a relatively stronger interaction than those formed from the SAN of 28% AN content.

Figures 1–7 show semilogarithmic plots of gas permeability coefficients P vs. volume fraction of SAN in the blend, ϕ_1, for the seven gases. As can be seen, the measured permeabilities for the blends are higher than those calculated from eq. (1) (shown by the dashed lines) whether the AN content in SAN is 13.5 or 28%. The lower permeabilities for the 28% AN blends than for the 13.5% AN blends are a result of the better barrier properties of polyacrylonitrile[24] compared to polystyrene. For O_2, CH_4, and CO_2, the curves represent permeabilities calculated from eq. (2) using A values of 7.9×10^{-7},[9] 2.2×10^{-6}, and 6.6×10^{-6},[25] respectively. The gas transport behavior in PMMA/SAN blends can be well described by eq. (2), which is not the case for other miscible blend systems previously studied.[1-10] For the other four gases,

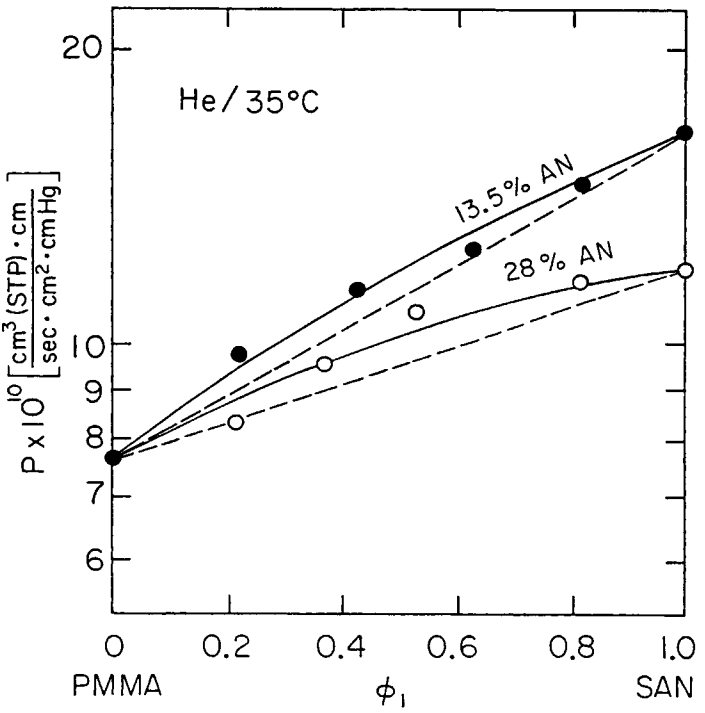

Fig. 1. Semilogarithmic plots of He permeability vs. volume fraction of SAN in homogeneous blends.

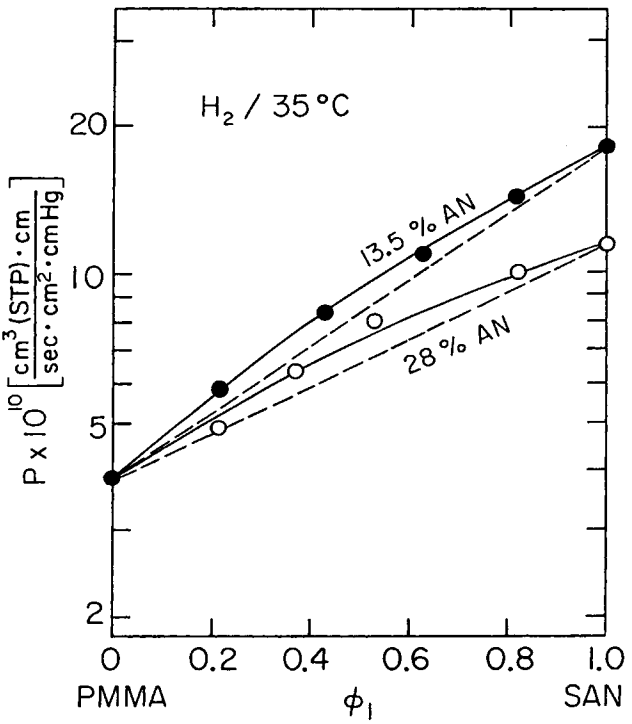

Fig. 2. Semilogarithmic plots of H_2 permeability vs. volume fraction of SAN in homogeneous blends.

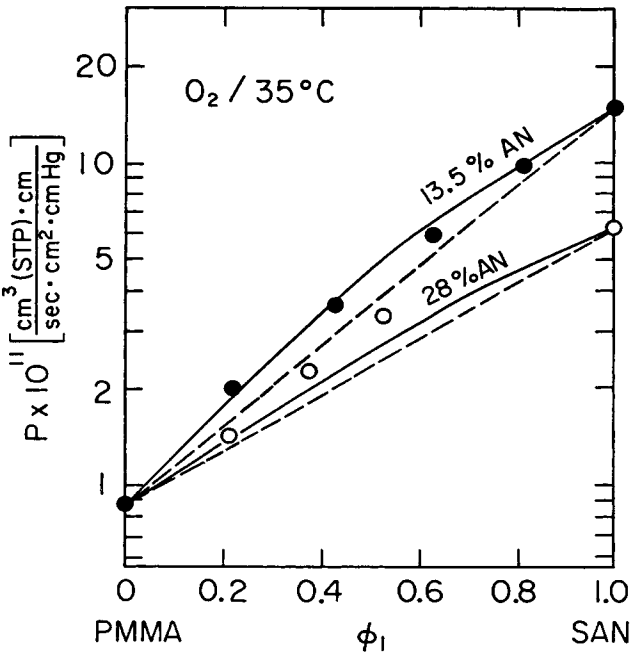

Fig. 3. Semilogarithmic plots of O_2 permeability vs. volume fraction of SAN in homogeneous blends.

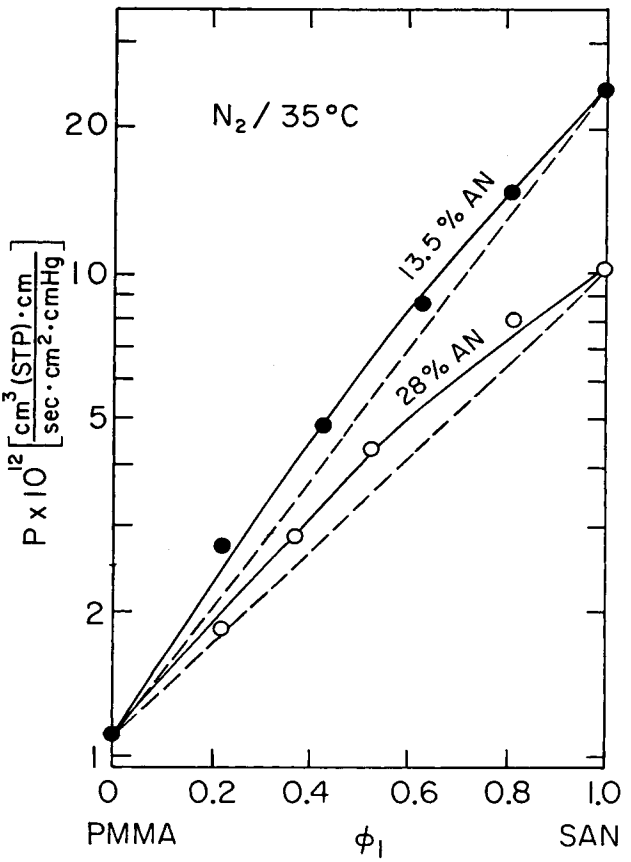

Fig. 4. Semilogarithmic plots of N_2 permeability vs. volume fraction of SAN in homogeneous blends.

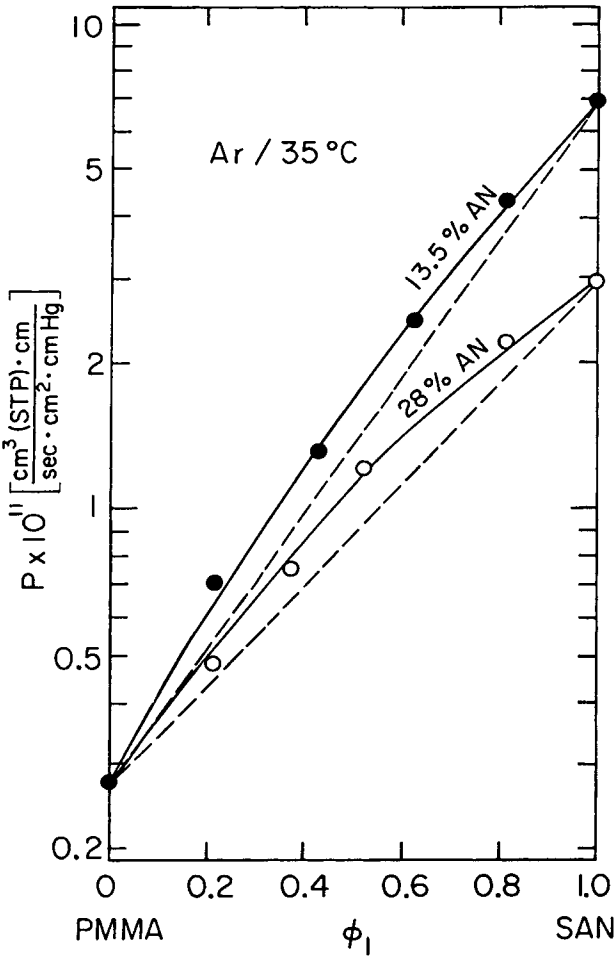

Fig. 5. Semilogarithmic plots of Ar permeability vs. volume fraction of SAN in homogeneous blends.

the curves were arbitrarily drawn to best fit the data because no A values are available.

Figures 8–12 show semilogarithmic plots of the apparent diffusion coefficients D_a, defined as

$$D_a = l^2/6\theta \tag{3}$$

vs. the blend composition, where l is the film thickness and θ is the diffusion times lag. Like the results for permeability coefficients, the measured diffusion coefficients are higher than predicted from the semilogarithmic additivity rule. This result is also contrary to several other miscible blend systems reported recently[1-10] which show diffusion coefficients either lower than or the same as that calculated from the semilogarithmic additivity rule.

The apparent solubility coefficient S_a for various gases defined as

$$S_a = P/D_a \tag{4}$$

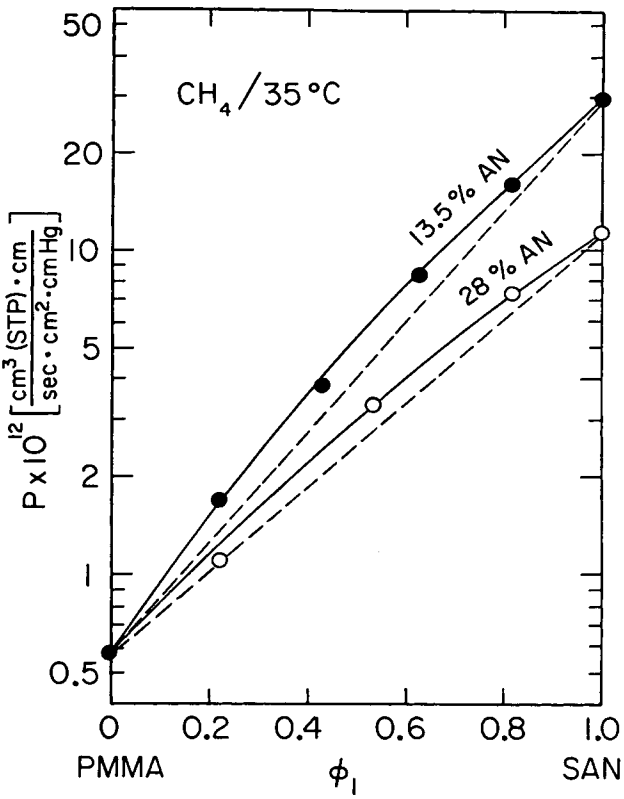

Fig. 6. Semilogarithmic plots of CH_4 permeability vs. volume fraction of SAN in homogeneous blends.

are plotted semilogarithmically vs. the blend composition in Figure 13. Within experimental error, a linear semilogarithmic relation is seen for all gases. Except for CO_2, a change of AN content from 13.5 to 28% does not affect the apparent solubility. The higher apparent CO_2 solubility coefficients in the 28% AN blends compared to the 13.5% AN blends do not necessarily mean higher CO_2 solubility in polyacrylonitrile than in polystyrene because the S_a defined in eq. (4) includes other dual mode sorption and dual mobility transport parameters[26] in addition to the Henry's solubility parameter k_D. Indeed, polyacrylonitrile has a lower k_D for CO_2 than does polystyrene.[2,27]

The composition dependence of transport properties shown above can also be explained in terms of the activated state theory,[9] which predicts diffusion of small molecules in a miscible blend to be given by

$$\ln D = \phi_1 \ln D_1 + \phi_2 \ln D_2 + (\alpha RT - 1)\Delta E_{12}/RT \tag{5}$$

where α is a constant which gives $(\alpha RT - 1)$ a negative value of approximately -0.5, R is the gas constant, T is the temperature, and ΔE_{12} is a deviation term for the activation energy, E_D, defined as

$$E_D = \phi_1 E_{D1} + \phi_2 E_{D2} + \Delta E_{12} \tag{6}$$

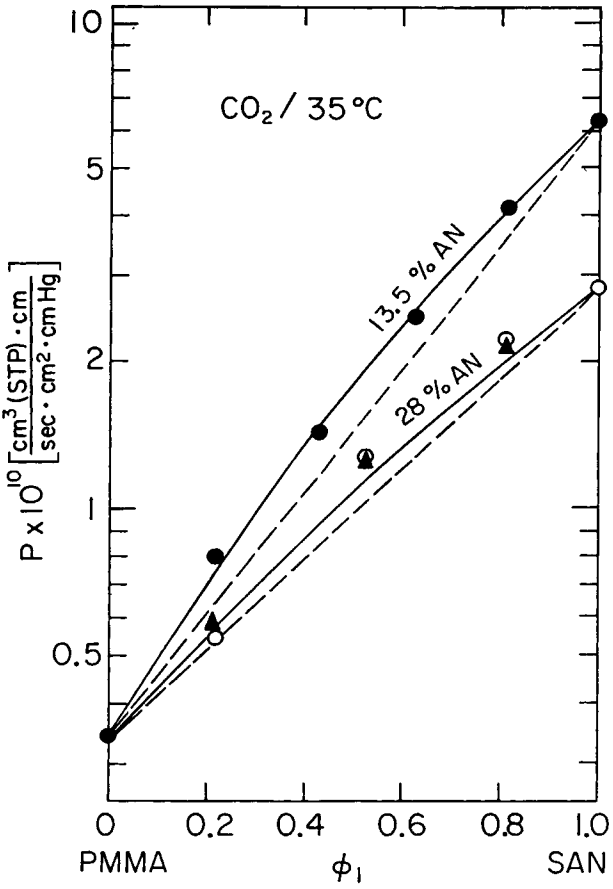

Fig. 7. Semilogarithmic plots of CO_2 permeability vs. volume fraction of SAN in homogeneous (○, ●) and phase-separated (▲) blends.

According to eq. (5), the positive deviation of diffusion coefficients shown in Figures 8–12 suggests a negative ΔE_{12}. In other words, the activation energy for gas diffusion in PMMA/SAN blends is smaller than the arithmetic sum for the two component polymers; or, relatively less energy is required for gas molecules to jump from one site to another when PMMA and SAN are mixed.

The composition dependence of solubility coefficients in a miscible blend can be analyzed by ternary solution theory[1,2,8] from which the gas solubility S in the blend can be related to that in the components

$$\ln S = \phi_1 \ln S_1 + \phi_2 \ln S_2 + (BV_3/RT)\phi_1\phi_2 \tag{7}$$

where B is the binary interaction parameter for the blend and V_3 is the molar volume of the gas. The semilogarithmic relation shown in Figure 13 suggests the last term in eq. (7) is close to zero, i.e., the binary interaction parameter B for PMMA/SAN blends is very small. This result is consistent with other results reported earlier such as lack of shift in the infrared spectrum when PMMA is mixed with SAN,[17] the heat of mixing of PMMA with SAN

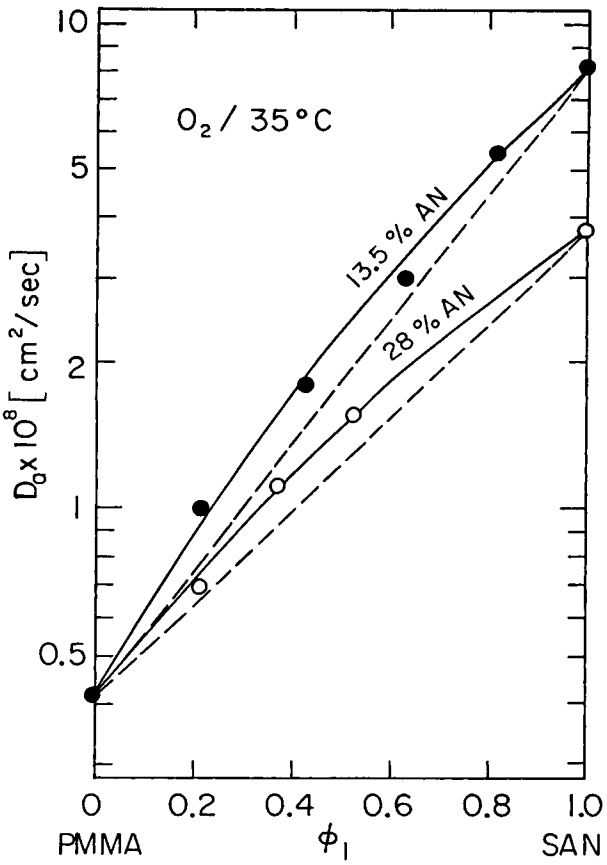

Fig. 8. Semilogarithmic plots of O_2 apparent diffusion coefficient vs. volume fraction of SAN in homogeneous blends.

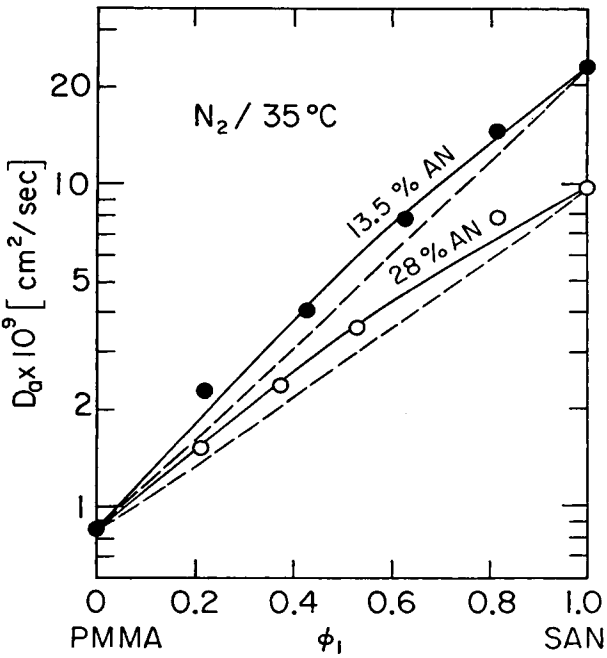

Fig. 9. Semilogarithmic plots of N_2 apparent diffusion coefficient vs. volume fraction of SAN in homogeneous blends.

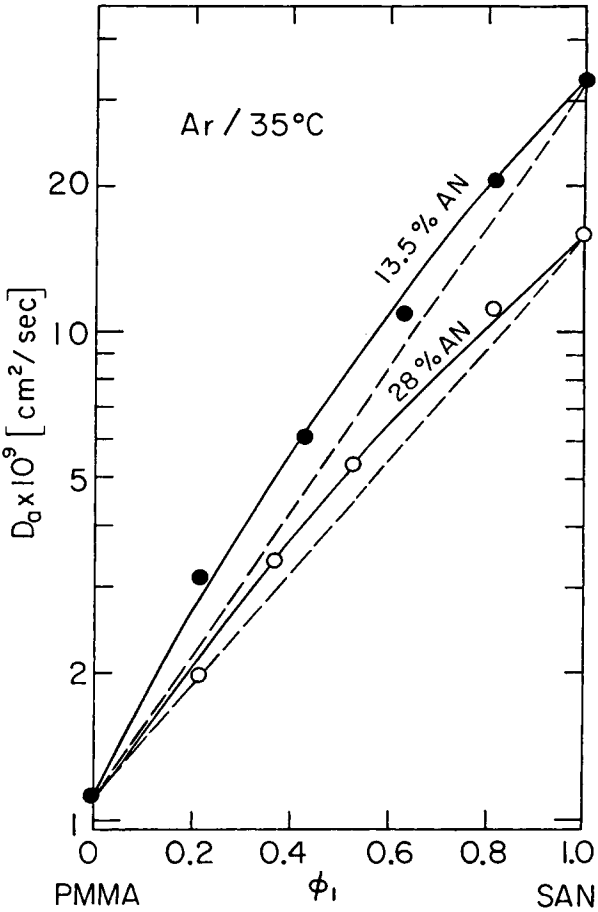

Fig. 10. Semilogarithmic plots of Ar apparent diffusion coefficient vs. volume fraction of SAN in homogeneous blends.

simulated by analog compounds is small although negative,[19] and zero excess volumes on mixing.[21]

Since the permeability coefficient is the product of diffusion and solubility coefficients, i.e., $P = DS$, the combination of eqs. (5) and (7) gives

$$\ln P = \phi_1 \ln P_1 + \phi_2 \ln P_2 + (\alpha RT - 1)\Delta E_{12}/RT + (BV_3/RT)\phi_1\phi_2 \quad (8)$$

Following the arguments given above, the positive deviation of permeability coefficients observed in Figures 1–7 must come from the extra diffusion term, ΔE_{12}, if eq. (5) is applicable.

Ideal Gas Separation Factor

Our recent studies on gas separation using miscible blend membranes have shown that the ideal gas separation factors for gas A relative to gas B defined as

$$\alpha_B^A = P_A/P_B \quad (9)$$

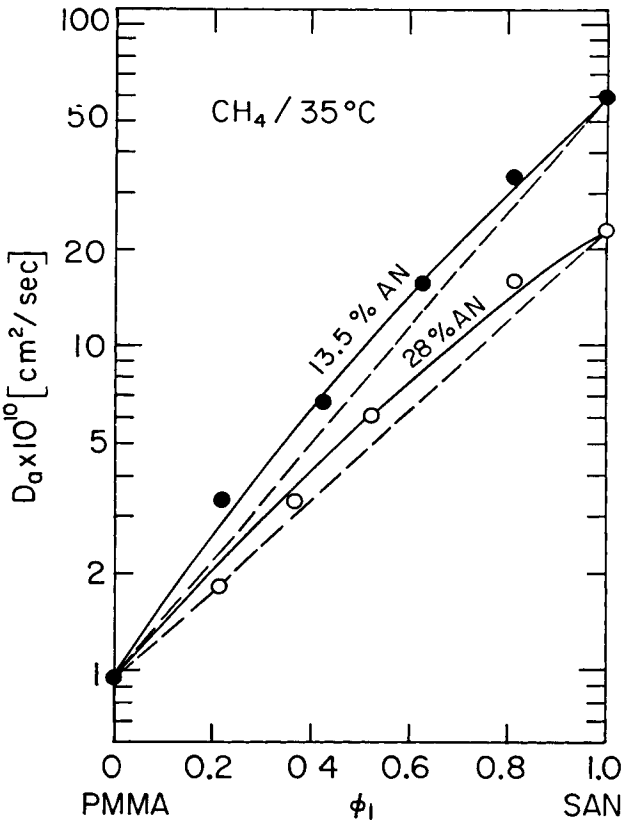

Fig. 11. Semilogarithmic plots of CH_4 apparent diffusion coefficient vs. volume fraction of SAN in homogeneous blends.

can be higher than that predicted from the semilogarithmic additivity rule, i.e.,

$$\ln \alpha_B^A = \phi_1 \ln(\alpha_B^A)_1 + \phi_2 \ln(\alpha_B^A)_2 \tag{10}$$

when the interactions between the two-component polymers in the blend are relatively strong.[3,6,7,10,11] Note that eq. (10) can be directly derived when gases A and B both follow eq. (1). In cases where the two-component polymers have strong interactions and similar separation factors, the separation factors for the blends may be even higher than that of the component polymers.[3,7,10,11] Thus, there is a potential advantage of using strongly interacting miscible blends for separating gases. Of course, it should be borne in mind that when the separation factor is enhanced, the absolute permeability coefficient is usually sacrificed to some degree.

In this study, the ideal separation factors for four gas pairs of some practical interest, namely, He/CH_4, H_2/CH_4, O_2/N_2, and CO_2/CH_4, are considered below to examine the blend permselectivity characteristics. Figures 14–16 show semilogarithmic plots of the ideal separation factors vs. the blend composition. As can be seen, linear relationships are observed for all gas pairs.

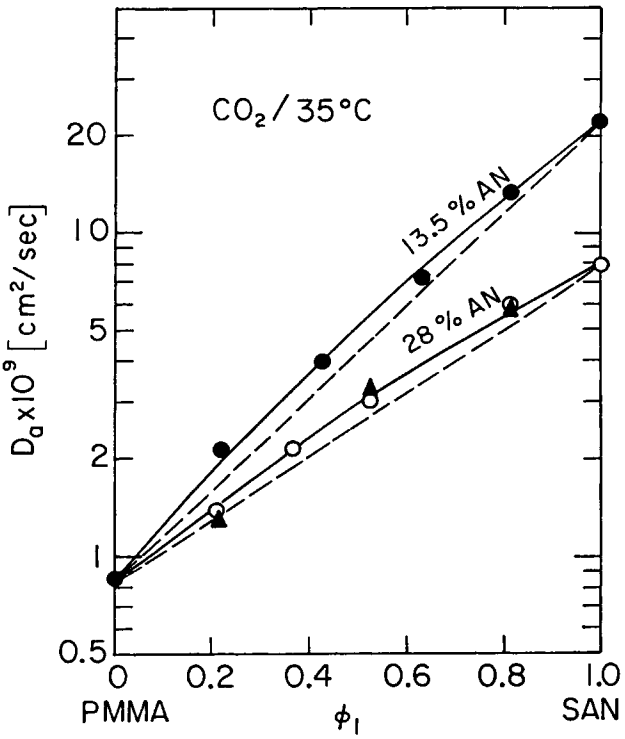

Fig. 12. Semilogarithmic plots of CO_2 apparent diffusion coefficient vs. volume fraction of SAN in homogeneous (○, ●) and phase-separated (▲) blends.

This result is different from what we have observed for strongly interacting blend systems which show better separation than eq. (10) predicts. Moreover, this result also suggests that the extent of positive deviations of gas permeabilities from eq. (1) is the same for all gases in PMMA/SAN blends, [otherwise eq. (10) is not followed]. Such a result is again contrary to that found for the other blend systems mentioned[3,6,7,10,11] which exhibit larger negative deviation of permeability from eq. (1) for gases of larger molecular size so that the deviation of separation factors from eq. (10) increases with the difference in molecular size of the two gas molecules.

Phase-Separated Blends

As mentioned, PMMA/SAN blends exhibit phase separation on heating or lower critical solution temperature behavior. A highly interconnected, two-phase structure can be formed when homogeneous PMMA/SAN blends are heated to temperatures just above their cloud points. This has been demonstrated using transmission electron microscopy[14] and laser light scattering.[20] In the following we will show that the same conclusion can be reached from measurement of gas transport properties.

In order to obtain phase-separated blends without overheating them to decomposition, only blends with 28% AN content were examined since blends of SAN with 13.5% AN have cloud points beyond 400°C. The homogeneous

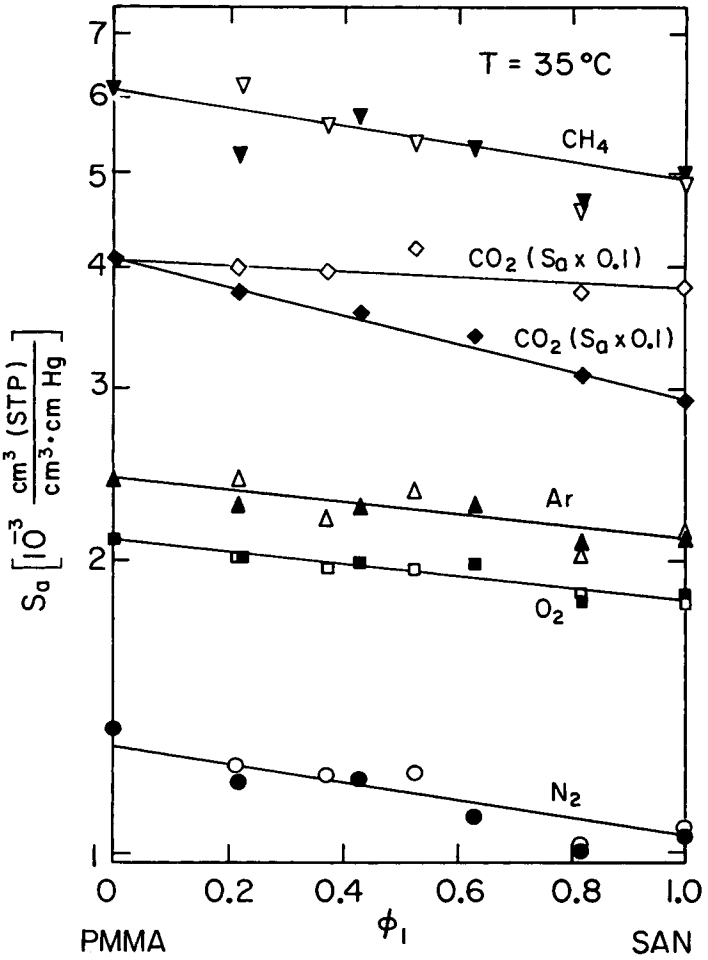

Fig. 13. Semilogarithmic plots of apparent gas solubility coefficients vs. volume fraction of SAN in homogeneous blends: (▽, ◇, △, □,○) 28% AN; (▼, ◆, ▲, ■, ●) 13.5% AN.

blends cast on glass plates with 20, 50, and 80% by weight of SAN were heated in an oven at 225, 215, and 260°C, respectively, or about 30–40°C higher than their corresponding cloud points, until they became cloudy. The films were then quenched to ambient conditions which does not permit return to a homogeneous state.

Although transport measurements were made for all gases with the phase-separated blends, only the results for CO_2 gas are discussed below since the findings are the same for all gases. The permeability and apparent diffusion coefficients of CO_2 in the phase-separated blends are shown in Figures 7 and 12, respectively (see the triangular symbols). The phase-separated blends have very similar transport properties as the homogeneous blends which is explained by the following analysis.

According to Kraus and Rollmann,[28] the elastic modulus of an isotropic, two-phase system can be calculated from the geometric models illustrated in Figure 17. Figure 17(A) represents an isotropic dispersion of component 2

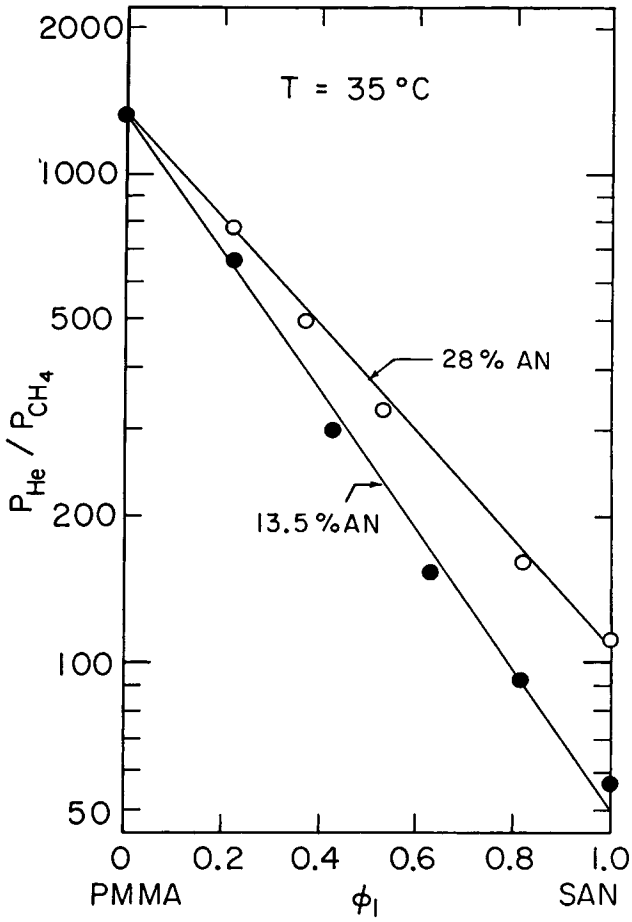

Fig. 14. Semilogarithmic plots of ideal separation factor for He/CH_4 pair vs. volume fraction of SAN in homogeneous blends.

(shaded part) in a mixture with component 1 having the unit dimensions shown there. Figures 17(B) and (C), respectively, exhibit two extreme ways to arrange the various elements, namely, series–parallel and parallel–series models. Notice that a limiting case of the dispersion of a two-phase system is an interpenetrating (or interconnecting) network where each component of the blend disperses throughout the other. This occurs when the dimension $b = 1$ in Figure 17(A). For this interconnected, two-phase structure, Kraus and Rollmann showed that the elastic modulus of the blend can be related to those of the two pure components, E_1 and E_2, and the dimension a by the following equations:

$$E = a^2E_2 + (1 - a)^2E_1 + \frac{2a(1 - a)}{(1 - a)/E_1 + a/E_2} \qquad (11)$$

(for parallel–series model)

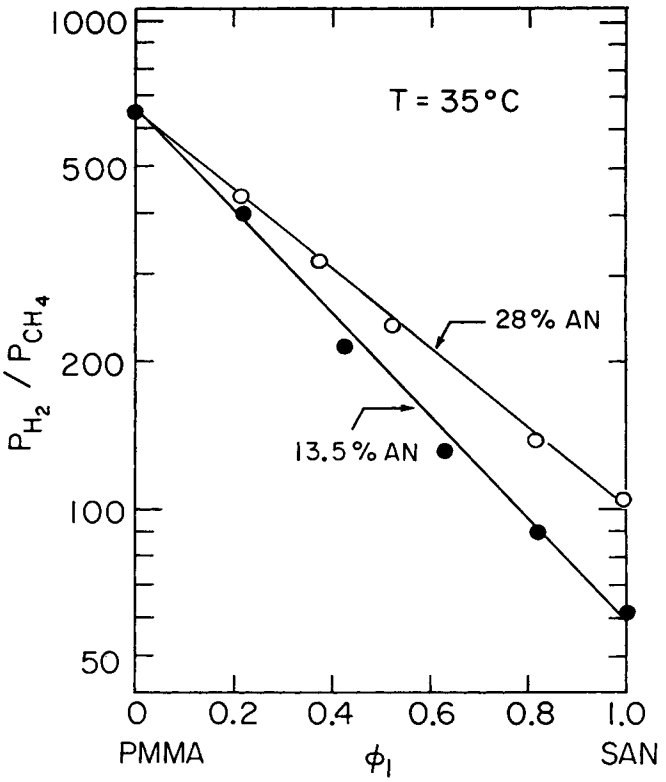

Fig. 15. Semilogarithmic plots of ideal separation factor for H_2/CH_4 pair vs. volume fraction of SAN in homogeneous blends.

and

$$E = \left[\frac{a}{a(2-a)E_2 + (1-a)^2 E_1} + \frac{1-a}{a^2 E_2 + (1-a^2)E_1} \right]^{-1} \tag{12}$$

(for series–parallel model)

The volume fraction of phase 1 in the blend ϕ_1, can be expressed as

$$\begin{aligned} \phi_1 &= 1 - \phi_2 \\ &= 1 - a^2(3 - 2a) \end{aligned} \tag{13}$$

Since the mechanical and the transport problems are mathematically similar, eqs. 11 and 12 are used to calculate the gas permeability by substitution of permeability P for modulus E. The dimension a for each blend composition can be simply determined from eq. (13) by knowing the volume fraction of component 1 (SAN) in the blend (see Table II). Using $P_1 = 2.84 \times 10^{-10}$ and $P_2 = 0.34 \times 10^{-10}$ [cm^3 (STP) cm/s · cm^2 · cm Hg] for CO_2 permeability in SAN and PMMA, respectively, CO_2 permeability coefficients in the three phase-separated blends were calculated and are compared with the experimen-

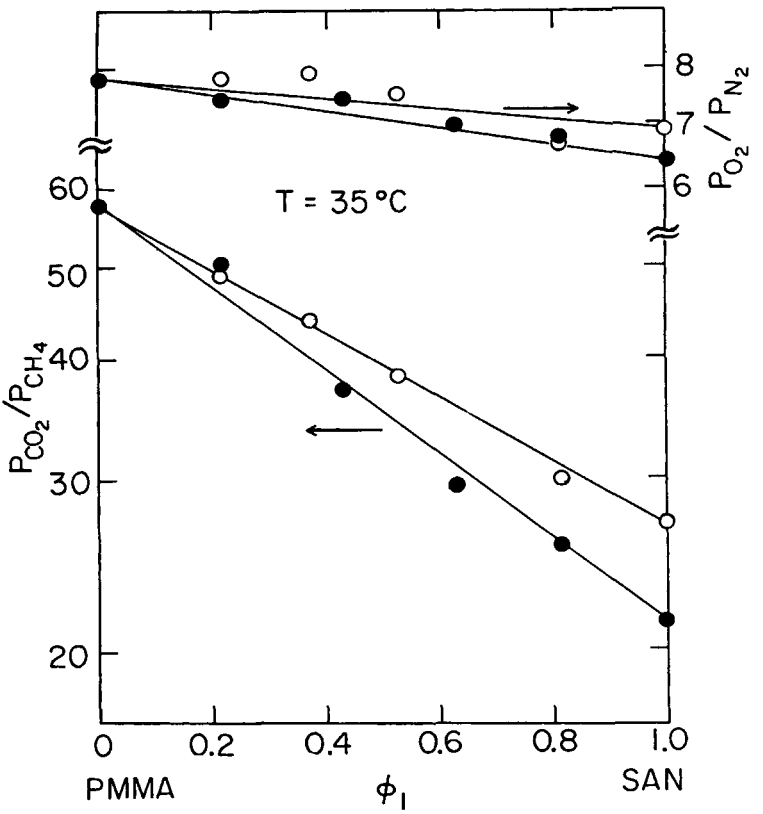

Fig. 16. Semilogarithmic plots of ideal separation factor for CO_2/CH_4 pair vs. volume fraction of SAN in homogeneous blends: (○) 28% AN; (●) 13.5% AN.

tal values in Table II. Both the series–parallel and the parallel–series models, with the assumption of interconnected structure, predict very closely the gas transport properties of these phase-separated SAN/PMMA blends.

The solubilities of CO_2 in both homogeneous and phase-separated blends are compared directly from their sorption isotherms in Figure 18. Since both samples have very similar permeability and diffusion coefficients (see Fig. 7 and 12), it is not surprising that their sorption isotherms are almost identical. The sorption parameters analyzed from the dual mode sorption equation

$$C = k_D p + C'_H bp/(1 + bp) \tag{14}$$

are $k_D = 0.89$ [cm³(STP)/(cm³ atm)], $C'_H = 16.6$ [cm³(STP)/cm³], and $b = 0.183$ atm^{-1}, where k_D is the Henry's law solubility, C'_H is the Langmuir site capacity, and b is the affinity constant.

Comparison of Gas Permeabilities for Solution-Cast and Melt-Extruded PMMA Films

It is well known that gas transport properties of glassy polymers are strongly affected by the methods of fabrication and any post-treatment they

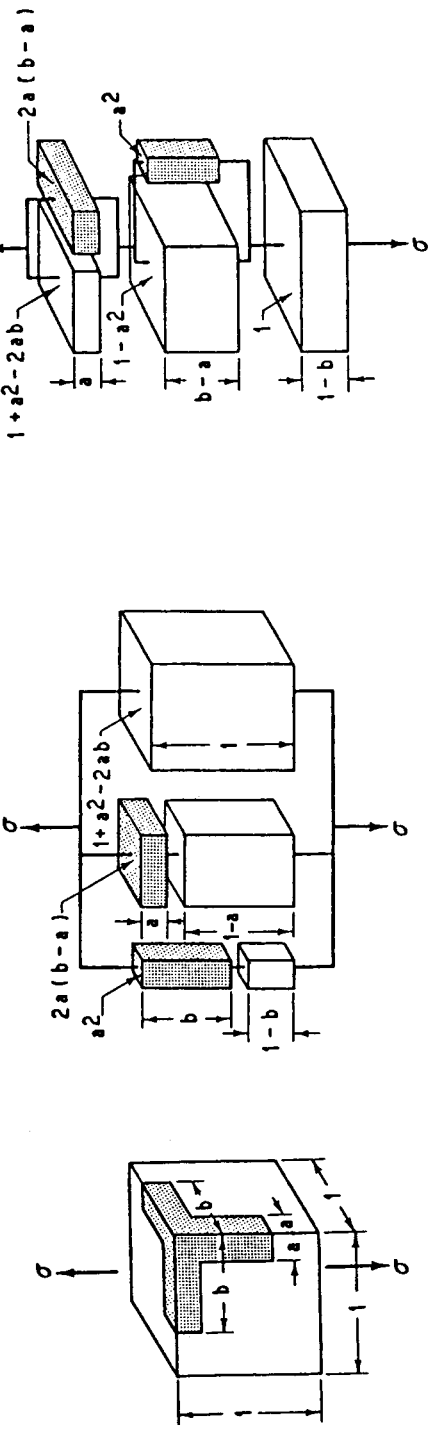

Fig. 17. Kraus and Rollmann's isotropic model for a polymer mixture: (A) elements of component 2 (shaded) in a mixture of unit volume; (B) series–parallel model. (C) parallel–series model. Note that $b = 1$ for an interconnected network.

TABLE II
Comparison of CO_2 Permeability Coefficients at 35°C in Phase-Separated PMMA/SAN (28% AN) Blends

Blend composition		$P \times 10^{10}$ [cm^3(STP) cm/s cm^2 cm Hg]		
		Calculated from Kraus and Rollmann model		
SAN/PMMA by wt	ϕ_1	Series parallel	Parallel series	Experimental
20/80	0.216	0.62	0.70	0.58
50/50	0.524	1.14	1.42	1.25
80/20	0.815	1.94	2.27	2.11

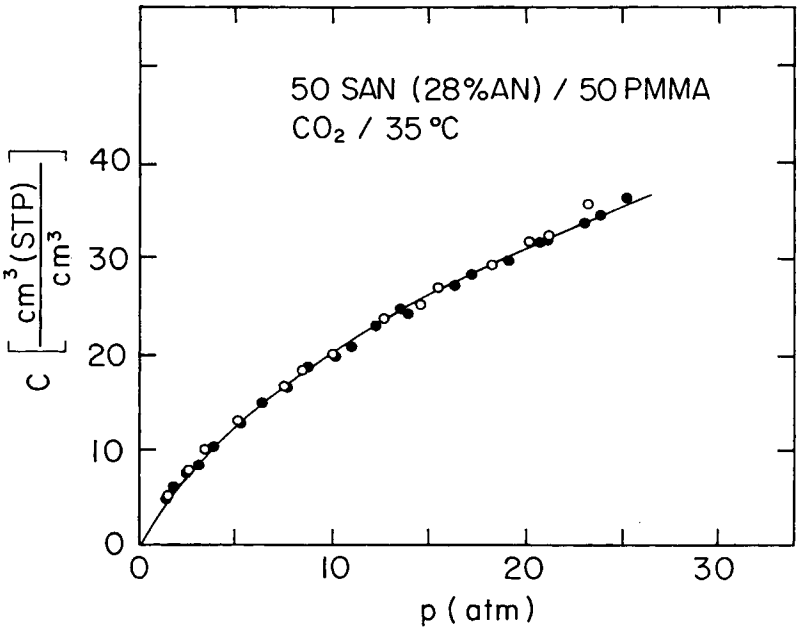

Fig. 18. Sorption isotherms for CO_2 in homogeneous (●) and phase-separated (○) 50 PMMA/50 SAN (28%AN) blends.

experience such as mechanical drawing or thermal annealing. The gas permeabilities for all samples reported here, including pure PMMA, were measured using solution cast films; however, a previous study of gas transport in blends of poly(vinylidene fluoride) with PMMA used melt extruded films,[6] which allows us to compare results for PMMA films made by these two methods. As seen in Table III, the extruded PMMA film has very similar gas permeabilities as the solution cast film for gases of relatively small size like He, H_2, and O_2. On the other hand, much smaller permeabilities are observed for the extruded film compared to the solution cast film for gases of relatively larger size like N_2 and CH_4. For example, the permeability to CH_4 for the cast PMMA film is a factor of 1.65 larger than for the extruded film (see the last column of Table III). Such results are consistent with those reported for other polymers[28-33] and can be attributed to the molecular orientation of the

TABLE III
Effect of Film Fabrication Method on Gas Permeabilities in PMMA at 35°C

Gas	Solution cast film P_S [a]	Extruded film P_E [a]	P_S/P_E
He	7.6×10^{-10}	7.6×10^{-10}	1.0
H_2	3.7×10^{-10}	3.7×10^{-10}	1.0
O_2	8.6×10^{-12}	8.7×10^{-12}	1.0
CO_2	3.4×10^{-10} [b]	3.1×10^{-10} [b]	1.10
Ar	2.7×10^{-12}	2.1×10^{-12}	1.29
N_2	1.1×10^{-12}	8.2×10^{-13}	1.34
CH_4	5.8×10^{-13}	3.5×10^{-13}	1.65

[a] All units in [cm^3(STP) cm/s cm^2 cm Hg)].
[b] Data taken at 1 atm.

extruded film. The fact that the effect of orientation on gas transport properties increases with the gas molecular size has been observed previously.[31,32] The very similar gas permeabilities for cast and extruded PMMA films for small gas molecules suggest that the orientation in the extruded film is rather low. Indeed, the birefringence of the extruded PMMA film is not significant.[6]

SUMMARY

This study has shown that gas transport behavior in miscible PMMA/SAN blends is different from many other miscible blend systems in several aspects. The gas permeability and diffusion coefficients for PMMA/SAN blends are somewhat higher than those calculated from the semilogarithmic additivity rule whereas the other miscible blends mentioned show a negative deviation from this rule or no deviation at all. On the other hand, the ideal gas separation factors for PMMA/SAN blends follow this rule well while the other miscible blends give higher separation factors than predicted. Alteration of the SAN comonomer composition from 28 to 13.5% by weight of AN which does affect the relative net interaction between PMMA and SAN does not lead to any change in this behavior. The behavior observed for PMMA/SAN blends is attributed to the very weak absolute net interaction between PMMA and SAN, regardless of AN content, as indicated by much other evidence and confirmed by the current gas solubility results. The second part of this series illustrates the effects of a stronger net interaction for a different homopolymer–copolymer blend system.[11]

The gas transport behavior in homogeneous PMMA/SAN blends are well explained by transport models derived from free volume theory, assuming no volume change on mixing or additive free volume. The gas transport behavior of phase-separated PMMA/SAN blends are well described by a two-phase, interconnected model proposed by Kraus and Rollmann.[28]

This research was supported by the U.S. Army Research Office and the Separations Research Program administered by the Center for Energy Studies at the University of Texas at Austin.

References

1. P. Masi, D. R. Paul, and J. W. Barlow, *J. Polym. Sci., Polym. Phys. Ed.*, **20**, 15 (1982).
2. G. Morel and D. R. Paul, *J. Membr. Sci.*, **10**, 273 (1982).
3. Y. Maeda and D. R. Paul, *Polymer*, **26**, 2055 (1985).
4. J. S. Chiou, J. W. Barlow, and D. R. Paul, *J. Appl. Polym. Sci.*, **30**, 1173 (1985).
5. J. S. Chiou and D. R. Paul, *J. Appl. Polym. Sci.*, **32**, 2897 (1986).
6. J. S. Chiou and D. R. Paul, *J. Appl. Polym. Sci.*, **32**, 4793 (1986).
7. A. Muruganandam, W. J. Koros, and D. R. Paul, to appear.
8. H. B. Hopfenberg and D. R. Paul, *Polymer Blends*, D. R. Paul and S. Newman, Eds., Academic, New York, 1978, Vol. I, Chap. 10.
9. D. R. Paul, *J. Membr. Sci.*, **18**, 75 (1984).
10. J. S. Chiou and D. R. Paul, *J. Appl. Polym. Sci.*, to appear.
11. J. S. Chiou and D. R. Paul, to appear.
12. W. M. Lee, *Polym. Eng. Sci.*, **20**, 65 (1980).
13. A. E. Barnabeo, W. S. Creasy, and L. M. Robeson, *J. Polym. Sci., Polym. Chem. Ed.*, **13**, 1979 (1975).
14. L. P. McMaster, *Adv. Chem. Ser.*, **142**, 43 (1975).
15. W. A. Kruse, R. G. Kirste, J. Haas, B. J. Schmitt, and D. J. Stein, *Makromol. Chem.*, **177**, 1145 (1976).
16. R. E. Berstein, C. A. Cruz, D. R. Paul, and J. W. Barlow, *Macromolecules*, **10**, 681 (1977).
17. K. Naito, G. E. Johnson, D. L. Allara, and T. K. Kwei, *Macromolecules*, **11**, 1260 (1978).
18. V. J. McBrierty, D. C. Douglass, and T. K. Kwei, *Macromolecules*, **11**, 1265 (1978).
19. J. -L. G. Pfennig, H. Keskkula, J. W. Barlow, and D. R. Paul, *Macromolecules*, **18**, 1937 (1985).
20. J. Kressler, H. W. Kammer, and K. Klostermann, *Polym. Bull.*, **15**, 113 (1986).
21. M. E. Fowler, J. W. Barlow, and D. R. Paul, *Polymer*, to appear.
22. W. J. Koros, D. R. Paul, and A. A. Rocha, *J. Polym. Sci., Polym. Phys. Ed.*, **14**, 687 (1976).
23. W. J. Koros and D. R. Paul, *J. Polym. Sci., Polym. Phys. Ed.*, **14**, 1903 (1976).
24. S. M. Allen, M. Fujii, V. Stannett, H. B. Hopfenberg, and J. L. Williams, *J. Membr. Sci.*, **2**, 153 (1977).
25. Y. Maeda, Ph D. dissertation, Univ. of Texas at Austin, 1986.
26. D. R. Paul and W. J. Koros, *J. Polym. Sci., Polym. Phys. Ed.*, **14**, 675 (1976).
27. G. S. Huvard, V. T. Stannett, W. J. Koros, and H. B. Hopfenberg, *J. Membr. Sci.*, **6**, 185 (1980).
28. G. Kraus and K. W. Rollmann, *Adv. Chem. Ser.*, **99**, 189 (1971).
29. R. E. Barker, R. C. Tsai, and R. A. Willency, *J. Polym. Sci., Polym. Symp. Ed.*, **63**, 109 (1978).
30. L. H. Wang and R. S. Porter, *J. Polym. Sci., Polym. Phys. Ed.*, **22**, 1645 (1984).
31. M. J. El-Hibri and D. R. Paul, *J. Appl. Polym. Sci.*, **30**, 3649 (1985).
32. M. J. El-Hibri and D. R. Paul, *J. Appl. Polym. Sci.*, **31**, 2533 (1986).
33. P. S. Holden, G. A. J. Orchard, and I. M. Ward, *J. Polym. Sci., Polym. Phys. Ed.*, **23**, 709 (1985).

Received November 11, 1986
Accepted January 13, 1987